Fungal Epithiodiketopiperazines Carrying α,β-Polysulfide Bridges from *Penicillium steckii* YE, and Their Chemical Interconversion

Guangde Jiang,[a] Peilan Zhang,[a] Ranjala Ratnayake,[a] Guang Yang,[a] Yi Zhang,[a] Ran Zuo,[a] Magan Powell,[a] José C. Huguet-Tapia,[b] Khalil A. Abboud,[c] Long H. Dang,[a, d] Max Teplitski,[e] Valerie Paul,[f] Rui Xiao,[g] K. H. Ahammad,[a] Uz Zaman,[h] Zhenquan Hu,[i, j] Shugeng Cao,[h] Hendrik Luesch,[a] and Yousong Ding*[a]

Some fungal epithiodiketopiperazine alkaloids display α,β-polysulfide bridges alongside diverse structural variations. However, the logic of their chemical diversity has rarely been explored. Here, we report the identification of three new (**2**, **3**, **8**) and five known (**1**, **4**–**7**) epithiodiketopiperazines of this subtype from a marine-derived *Penicillium* sp. The structure elucidation was supported by multiple spectroscopic analyses. Importantly, we observed multiple nonenzymatic interconversions of these analogues in aqueous solutions and organic solvents. Furthermore, the same biosynthetic origin of these compounds was supported by one mined gene cluster. The dominant analogue (**1**) demonstrated selective cytotoxicity to androgen-sensitive prostate cancer cells and HIF-depleted colorectal cells and mild antiaging activities, linking the bioactivity to oxidative stress. These results provide crucial insight into the formation of fungal epithiodiketopiperazines through chemical interconversions.

[a] *G. Jiang, P. Zhang, Dr. R. Ratnayake, Dr. G. Yang, Y. Zhang, R. Zuo, M. Powell, Prof. Dr. L. H. Dang, K. H. Ahammad, Prof. Dr. H. Luesch, Prof. Dr. Y. Ding*
Department of Medicinal Chemistry
Center for Natural Products, Drug Discovery and Development
University of Florida
Gainesville, 32610, FL (USA)
E-mail: yding@cop.ufl.edu
[b] *Dr. J. C. Huguet-Tapia*
Department of Plant Pathology, University of Florida
Gainesville,32611, FL (USA)
[c] *Dr. K. A. Abboud*
Department of Chemistry, University of Florida
Gainesville,32611, FL (USA)
[d] *Prof. Dr. L. H. Dang*
Department of Medicine, University of Florida
Gainesville,32610, FL (USA)
[e] *Prof. Dr. M. Teplitski*
Soil and Water Science Department, University of Florida
Gainesville,32610, FL (USA)
[f] *Dr. V. Paul*
Smithsonian Marine Station at Ft.Pierce
701 Seaway Drive, Ft. Pierce,34949, FL (USA)
[g] *Prof. Dr. R. Xiao*
Departments of Aging and Geriatric Research
Pharmacology and Therapeutics, Center for Smell and Taste
University of Florida
Gainesville,32610, FL (USA)
[h] *U. Zaman, Prof. Dr. S. Cao*
Department of Pharmaceutical Sciences
Daniel K. Inouye College of Pharmacy, University of Hawai'i at Hilo
Hilo, Hawaii 96720 (USA)
[i] *Prof. Dr. Z. Hu*
Warshel Institute for Computational Biology
The Chinese University of Hong Kong,Shenzhen, Guangdong, 518172, (P. R. China)
[j] *Prof. Dr. Z. Hu*
School of Chemistry and Materials Science
University of Science and Technology of China,
Hefei, Anhui, 230026, (P. R. China)

Supporting information for this article is available on the WWW under https://doi.org/10.1002/cbic.202000403

Introduction

Epithiodiketopiperazines (ETPs) are a family of fungal cyclic dipeptides featured by intramolecular polysulfide bridges, typically between two α-carbons.[1] These compounds possess substantial chemical diversity that is sparked by two modules of nonribosomal peptide synthetases (NRPSs) and a diverse set of tailoring enzymes.[2] Furthermore, ETPs possess an attractive spectrum of biological activities, such as antimicrobial, anticancer, and anti-inflammatory effects.[1] A unique subtype of bioactive fungal ETPs carries a -S-, -SS-, or -SSS- bridge between the α and β carbons and often contains an uncommon 1,2-oxazadecaline moiety (e.g., FA-2097, pretrichodermamides, outovirins, and adametizines; Figure 1 and Figure S1 in the Supporting Information).[3] Notably, members of this subtype also carry tailoring modifications on C6 and C7, including epoxidation, halogenation, and hydroxylation (Figure 1). However, the molecular bases of the formation of the α,β-polysulfide bridges and tailoring modifications remain mostly unclear.[2,4]

In our characterization of microbial communities associated with the coral black band disease,[5] a fungal strain YE was isolated from an infected *Pseudodiploria strigosa* coral collected at Looe Key Reef, FL, USA. Its internal transcribed spacer region (GenBank ID: KY750301) shared a 99.5% identity with *Penicillium steckii* KUC1681-1.[6] Chemical investigation of the fungal fermentation culture led to the identification of three new ETP analogues, named penigainamide A–C (**2**, **3**, and **8**, Figure 1), along with five known ones, adametizine A (*N*-methylpretrichodermamide B, **1**),[3f,g] FA2097 (**4**),[3c] outovirin A (**5**) and C (**6**),[3h] and pretrichodermamide C (**7**),[3f] all of which carry an α,β-polysulfide bridge and modifications on C6 and C7.

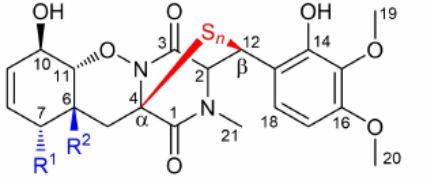

	R^1	R^2	n
Adametizine A (**1**):	Cl	OH	2
Penigainamide A (**2**):	Cl	OH	3
Penigainamide B (**3**):			1
FA-2097 (**4**):			2
Outovirin A (**5**):	OH	OH	1
Outovirin C (**6**):	OH	OH	3
Pretrichodermamide C (**7**):	OH	OH	2
Penigainamide C (**8**):	Cl	OH	1
Penigainamide D (**9**):			3

Figure 1. Chemical structures of penigainamides A–D and five known ETPs (**1** and **4–7**) carrying α, β-polysulfide bridges (in red) and modifications on C6 and C7 (in blue).

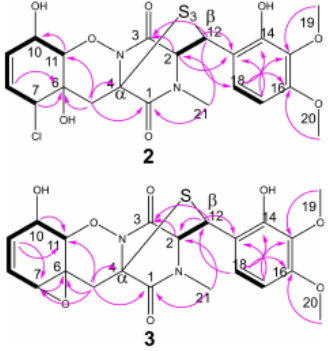

Figure 2. Key HMBC (arrows in pink) and COSY (bold lines) correlations of compounds **2** and **3**.

Many identified ETPs were unstable in aqueous solutions and organic solvents and can do interconvert. Herein, we present identification, structure elucidation, and interconversions of these analogues. A putative biosynthetic pathway is proposed on the basis of a gene cluster mined from the sequenced genome of *P. steckii* YE, and the cytotoxicity to cancer cells and antiaging activities of the major metabolite **1** are discussed.

Results and Discussion

Compound **1** was isolated as a colorless solid and its molecular formula was calculated as $C_{21}H_{23}ClN_2O_8S_2$ with HRMS analysis (*m/z* 531.0660 $[M+H]^+$, Figure S2). Its ^{1}H, ^{13}C and 2D NMR spectra and X-ray structure resembled reported data of adametizine A (*N*-methylpretrichodermamide B) with a determined absolute configuration (Figures S3–S9 and Table S1).

Penigainamide A (**2**) and B (**3**) were isolated as colorless solids. HRMS analysis indicated that **2** differs from **1** by one additional sulfur atom (*m/z* 563.0233 $[M+H]^+$), while its HRMS spectrum revealed the characteristic isotope pattern of a single chlorine atom (Figure S10). Compound **2** in multiple deuterated solvents (e.g., [D_6]acetone) experienced significant degradation within 30 minutes at room temperature, and its ^{1}H, ^{13}C, COSY, HSQC, and HMBC NMR spectra were eventually taken in CD_3OD at - 20 °C, which together led to the elucidation of its structure as shown (Figures 1, 2, and S11–S15, Table S2). The ^{1}H and ^{13}C NMR spectroscopic data indicated the presence of one *N*-methyl and two methoxy groups, one sp^3 methylene, four sp^2 and five sp^3 methines, and eight unprotonated (six sp^2 and two sp^3) carbon atoms. The assignment of the oxazine-cyclohexene moiety in **2** was supported by chemical shifts of two vinylic protons at δ 5.68 and δ 5.69 and one methylene group at δ = 2.27 and 2.80 (Table S2), C7- H/C8- H/C9- H/C10- H/C11- H COSY correlations, and HMBC correlations from C8- H to C6, C7- H to C6, and C5- H to C4/C6/C11 (Figure 2). Two *ortho* coupled aromatic protons at δ = 7.02 (*J* = 8.9 Hz, C17- H) and δ = 6.50 (*J* = 8.8 Hz, C18- H) and HMBC correlations of C18- H to C14 and C16, C17-H to C13 and C15, C19- H to C19, and C20- H to C20 suggested the presence of 2,3-dimethoxyphenol ring unit in **2**. Furthermore, the diketopiperazine core was assigned with the characteristic chemical shifts of carbonyl groups at δ = 164.7 (C2) and 164.2 (C3), the *N*-methyl group at δ = 3.31 (C21- H), and multiple HMBC correlations (C21- H to C1/C2, C2- H to C3, C12- H to C3/C13/C18, Figure 2). The structural elucidation of **2** was further supported by comparing the 1D NMR data of **1** (in CD_3OD at - 20 °C, Figures S16–S17), **2** and one known, structurally similar ETP analogue outovirin C (in CD_3OD at room temperature) that carries a trisulfide bridge (Table S2).[3h] The 1D NMR data of these three analogues were highly similar (Table S2), indicating the same skeleton. On the other hand, the chemical shifts of C12 and C12- H of **2** and outovirin C were clearly higher than **1** (C12: δ = 57.2 vs 56.3 vs 42.9; C12- H: δ = 5.51 vs 5.53 vs 4.62), suggesting the effects of the polysulfide bridge. Similarly, we observed the higher chemical shifts of C4 of **2** and outovirin C than **1** (C4: δ = 77.3 vs 76.7 vs 70.9). Furthermore, the - Cl substitution at C7 of **1** and **2** presumably led to the lower carbon chemical shift than the C7- OH containing outovirin C (C7: δ = 67.5 vs 66.8 vs 74.5). Compound **2** showed negative Cotton effects at 216 nm (- 3.85) and 262 nm (- 2.56), which closely resembled the reported data of **1** (Figure S18),[3g,7] and exhibited the same sign of optical rotation ($[\alpha]_D^{20}$ = - 281 (*c* 0.027, MeOH)) as **1**,[3g,7] indicating that **2** could have the same absolute configuration as **1**. The conversion of **1** to **2**, as discussed below, further suggested the same absolute configuration of these two ETP analogues.

The structure of **3** was elucidated on the bases of the HRMS spectrum (*m/z* 463.1158 $[M+H]^+$) and a set of ^{1}H, ^{13}C, COSY, HSQC, and HMBC NMR analysis (Figures 1, 2, and S19–S24, Table S3). Similar to **2**, the 1D NMR data of **3** indicated the presence of one *N*-methyl and two methoxy groups, one sp^3 methylene, four sp^2 and five sp^3 methines, and eight unprotonated (six sp^2 and two sp^3) carbon atoms. We further compared the 1D NMR data of **1** (in [D_6]DMSO, Figures S6 and S7), **3** (in [D_6]DMSO) and one known, structurally similar ETP analogue FA2097 (in [D_6]DMSO, Figure 1). Despite the high overall similarities (Table S3), the chemical shifts of C12 and C12- H of **3**

were notably higher than **1** and FA2097 (C12: $\delta = 47.0$ vs 41.0 vs 40.2; C12- H: $\delta = 5.45$ vs 4.62 vs 4.48), both of which carry a α,β-S_2 bridge, whereas its C4 was slightly lower (C4: $\delta = 67.8$ vs 69.1 vs 70.0). The chemical shifts of C12, C12-H and C4 of **1**, **2**, **3**, FA2097 and outovirin C were summarized in Table S4 and suggested that the higher sulfur number in the bridge likely induces a higher chemical shift of C4 but a mixed effect on C12 and C12- H. Besides, the epoxide on C6 and C7 of **3** and FA2097 clearly lowered the chemical shifts of these two positions, compared with **1**, **2**, and outovirin C (Tables S2 and S3). The structural assignment of **3** was further supported by its COSY and HMBC correlations that are similar to **1** and **2** (Figures 1, 2 and S8). Of note, **3** was unstable in multiple deuterated solvents even at - 20 °C. Although the absolute configuration of **3** was not determined, it could be the same as **1** due to likely sharing the same biosynthetic pathway and observed conversion of **1** to **3**.

When fermented for 14 days, *P. steckii* YE produced five additional ETPs carrying the α,β-polysulfide bridge, including four known compounds FA2097 (**4**), outovirin A (**5**) and C (**6**), and pretrichodermamide C (**7**) and one new ETP, named penigainamide C (**8**; Figure 3A). All known compounds showed the expected molecular weights in HRMS analysis and followed a characteristic MS/MS fragmentation pattern typical of this subtype of ETPs (Figures S25–S28).[3h] The *m/z* values of the fragment I reflect the number of its sulfur atoms, while those of the fragment II differ only by the chemical modifications on C6 and C7 (Figure 3B). Compounds **1**–**7** all showed the expected *m/z* values of the corresponding fragments I and II in tandem MS analysis (Figures S2, S10, S19, and S25–S28). The HRMS analysis revealed the isotope pattern of a single chlorine atom and suggested the molecular formula of **8** as $C_{21}H_{23}ClN_2O_8S$ (*m/z* 499.0813 $[M+H]^+$; Figure S29). The fragments I and II of **8** at *m/z* 199.0412 and 301.0582, respectively, indicated the presence of a monosulfide bridge and the C7–Cl substitution (Figure S29). NMR analysis of **8** was unsuccessful due to its rapid transformation into **3** in multiple deuterated organic solvents at room and low temperature (Figure 4A and S30).

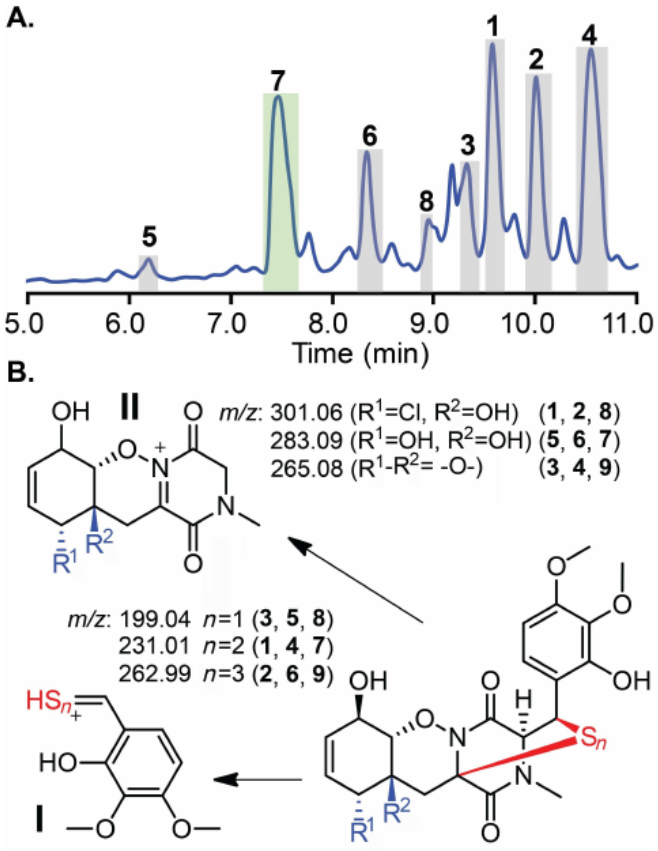

Figure 3. A) The HPLC trace of EtOAc crude extract of a 14-day fungal fermentation revealed three new (**2**, **3**, and **8**) and five known (**1**, and **4**–**7**) ETP analogues. Compound **7** was co-eluted with one unknown chemical and was identified by MS. B) The characteristic fragmentation pattern of ETPs with the α,β-polysulfide bridge delivered structural information.

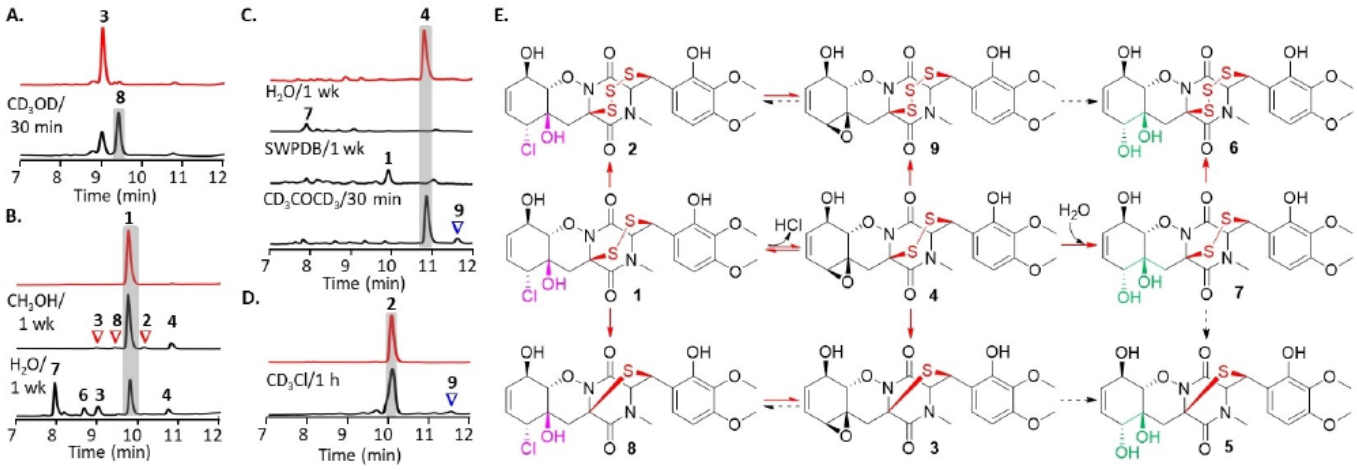

Figure 4. HPLC analysis of chemical transformations of A) **3**, B) **1**, C) **4**, and D) **2** into other ETPs under indicated conditions. All newly generated ETPs were confirmed by HRMS and tandem MS analysis. Small peaks are indicated with red or blue arrows. Standards are shown as red traces, and substrate peaks are shaded in gray; wk: week. E). Putative chemical transformation pathway of ETPs identified from the crude extract of *P. steckii* YE fermentation. Confirmed transformation steps are indicated with red arrows; the dashed arrows represent proposed reactions. Of note, besides the interconversions, in solution all of these ETPs can decompose at room temperature over time.

We further investigated the instability of the isolated ETPs. A small portion (~5%) of **1** was transformed into **2**, **3**, **4**, and **8** when dissolved in methanol for one week, while about 55% of **1** in MQ water was transformed mainly into **7** along with **3**, **4** and **6** as minor metabolites (Figures 4B and S31). Furthermore, **1** was relatively stable in acidic solutions but rapidly decomposed into a complicated, unidentifiable mixture under basic conditions. We propose that in addition to decomposition,[3c] two molecules of **1** can be transformed into one molecule of **8** with the monosulfide bridge and one molecule of **2** with the tri-sulfide bridge through a proposed path detailed in Figure S32, which is likely shared by the formation of outovirin analogues[3h] and some ETPs with the α,α-polysulfide bridge (e.g., sirodesmins and chetomins[8]). Of note, the stereochemical control of the newly formed polysulfide bridge through this pathway requires further detailed characterization, while the polysulfide bridges of all naturally isolated ETPs are in the eclipsed conformation. Recent work suggested strong n→π* interactions raised from the overlap of the p-type lone pairs of the sulfur atoms with the π* orbitals of the amide carbonyl group may dictate the formation of eclipsed conformation.[9] Furthermore, the interconversion of chlorination, epoxidation, and hydroxylation modifications on C6 and C7 of **1**, **2**, and **8** can occur to form **3**, **4**, **6**, and **7** (Figures S31 and S33). Similarly, isolated **4** was transformed completely in MQ water and potato dextrose broth prepared in artificial seawater (SWPDB) within one week, while forming only low levels of **7** and **1**, respectively (Figures 4C and S34). Shortly after dissolving **4** in [D_6]acetone, we observed the formation of a new ETP analogue (**9**) with a calculated molecular formula of $C_{21}H_{22}N_2O_8S_3$ (*m/z* 527.0609 [*M* + H]$^+$) in the HRMS analysis (Figures 4C, S35, and S36). The fragments I and II of **9** showed *m/z* values of 262.9865 and 265.0818 (Figure S36), indicating the presence of the α,β-trisulfide bridge and one epoxide on C6 and C7 (Figure 4E). This compound was also formed from **2** shortly after dissolving it in $CDCl_3$ for 1 hour (Figures 4D and S35) and is named as penigainamide D (**9**). Collectively, these results, for the first time, disclose the complicated interconversions of one subtype of ETPs through simultaneously nonenzymatic transformations of α,β-polysulfide bridge and epoxide/chlorohydrin/vicinal diols on C6 and C7 (Figure 4E), and expands known chemical transformations for the formation of natural product artifacts.[10] Of note, only **1** was detected from the EtOAc crude extract of two frozen black band layer samples (Figure S37), thus indicating its relatively high chemical stability.

To obtain new insights into the formation of isolated ETPs from *P. steckii* YE, we sequenced and assembled the fungal genome to provide 33.2 Mbp (781 contigs, 45.9% GC). Bioinformatics analysis revealed a 53-kb gene cluster (*pen*) that shares high similarity to the gliovirin gene cluster in *Trichoderma virens* (Figure 5 and Table S5).[11] Specifically, an NRPS (PenP) contains a single adenylation (A) domain with a predicted substrate preference to L-Phe and may form cyclo-[L-Phe-L-Phe] (Figure 5). The formation of the α,α-epidiothio bridge of ETPs has been well elucidated in the biosynthesis of gliotoxin.[2,12] It relies on a P450 (GliC) for two α-hydroxylations and a glutathione *S*-transferase (GliG) for the formation of a bisglutathione intermediate, whose stepwise degradation to the thiols requires a γ-glutamyl cyclotransferase (GliK), a dipeptidase (GliJ), and a C-S lyase (GliI). The formation of the bisthiol is then catalyzed by a flavin-dependent oxidase (GliT). The *pen* cluster encodes the full set of the above-mentioned enzymes (PenC, PenIJK and PenT) but also one additional PenT homolog (PenT*) and five extra P450s (Figure 5 and Table S5). Presumably, PenC and one of these additional P450s catalyze α- and β-hydroxylations, and PenIJK, PenT and PenT* together form the α,β-polysulfide bridge in the biosynthesis of penigainamides (Figure 5). Subsequently, one *N*-hydroxylation and one epoxidation on C10 and C11, which can be catalyzed by the P450 PenF and another P450, can lead to the formation of the 1,2-oxazadecaline moiety.[3b,12a] Compound **4** can be produced after serial tailoring enzymatic reactions, including aryl hydroxylations and epoxidation, N- and O-methylations, and can be further transformed to penigainamides and other known ETPs in a nonenzymatic manner (Figures 4 and 5, Table S5). Future studies will test this proposed biosynthetic pathway and clarify the order of key enzymatic steps. Importantly, genome-based searches showed that the *pen* cluster is present in several other fungal species, for example, the human pathogen *Aspergillus udagawae* (Figure S38).

The most stable and abundant ETP analogue of this work, **1**, possessed weak antimicrobial activity toward *Escherichia coli*,

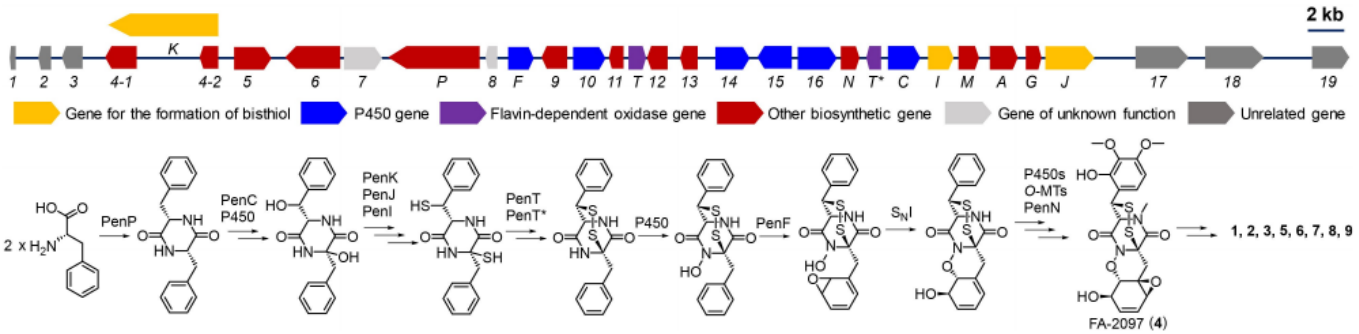

Figure 5. A proposed biosynthetic pathway of **1**–**9**. The *pen* gene cluster (top) was identified from the assembled genome of *P. steckii* YE. Predicted boundary genes are in gray; *pen7* and *pen8* are in light gray as their encoded products might not directly contribute to the biosynthesis of penigainamides. The predicted functions of the biosynthetic enzymes, the previous biosynthetic studies of ETPs, and the interconversions of identified EPTs carrying the α,β-polysulfide bridge in the current work support the proposed biosynthetic pathway.

Staphylococcus aureus, and *Candida albicans* at 10 μM (data not shown). Despite its weak cytotoxicity toward human cervical cancer HeLa cells at 10 μM, **1** showed activity toward PC-3 and LNCaP cells with IC_{50} of 6.3 ± 1.4 and 0.5 ± 0.03 μM, respectively, indicating about ten times higher cytotoxicity toward androgen-sensitive prostate cancer cells (Figure S39A). Compound **1** was also active against human colon cancer HCT116 cells with IC_{50} of 10.9 ± 0.9 μM and showed statistically significant higher sensitivity toward HCT116$^{HIF\text{-}1\alpha\text{-}/\text{-}\ HIF\text{-}2\alpha\text{-}/\text{-}}$ cells (IC_{50} 3.3 ± 0.5 μM, Figure 6A) whose hypoxia-inducible factors (HIF)-1α and - 2α genes are knocked out.[13] This result suggests a potential link between oxidative stress and the cytotoxicity of **1**, and the increased potency of **1** toward HIF-deficient HCT116 cells is strikingly different from other bioactive natural products we previously characterized (e.g., dolastatins 10/15 and largazole).[13–14] Furthermore, **1** was evaluated with the free-living soil nematode *Caenorhabditis elegans*. Interestingly, the worm showed a statistically significant preference for the food mixed with **1** at a high concentration (2 mM; Figure S39B), which further indicated the low-to-no cytotoxicity of **1** to normal cells.[15] At 100 μM, **1** prolonged the lifespan of animals by 9.1% compared to the blank control group (Figure 6B), suggesting a mild antiaging activity. The aging process of *C. elegans* shares many similarities to mammals, making it a common model animal for aging research.[16] Determination of detailed mechanisms of **1**'s actions awaits further studies. Bioactivities of other ETP analogues isolated in this work were not assessed due to limited quantities and stability concerns.

Conclusion

In summary, we have identified three new and five known ETPs carrying the distinct α,β-polysulfide bridge. The compounds were obtained from *P. steckii* YE, which was isolated from a black band disease sample. A combination of HRMS and 1D and 2D NMR spectral analyses led to the structural elucidation of penigainamides A and B (**2**, **3**). Multiple lines of evidence suggested the same absolute configuration of adametizine A (**1**) and **2**. Tandem MS analysis further aided the identification of four additional known ETPs (**4**–**7**) and penigainamide C (**8**). Surprisingly, these identified ETPs underwent interconversions in different aqueous solutions and solvents, leading to the identification of penigainamide D (**9**) by HRMS and tandem MS analysis. We proposed a biosynthetic pathway of **1**–**9**, which was supported by the *pen* gene cluster mined from the assembled genome of *P. steckii* YE and previous biosynthetic studies of other ETPs (e.g., gliotoxin). Moreover, **1** shows higher cytotoxicity toward androgen-sensitive prostate cancer cells and HIFs knockout colon cancer cells, suggesting the potential effects of oxidative stress on its bioactivity. Interestingly, **1** possesses mild antiaging activity with the *C. elegans* animal model. To our knowledge, **1** is the first ETP analogue demonstrating the *in vivo* antiaging activity, although the detailed mechanism is still unclear. These studies provide novel insights into the chemical logic of this subtype of ETPs,[4] and lay the groundwork for investigation of the chemical and functional diversity of fungal ETP alkaloids.[1,17]

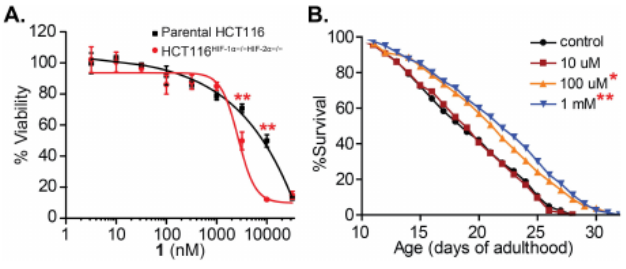

Figure 6. A) Compound **1** demonstrated a higher potency toward HCT116$^{HIF\text{-}1\alpha\text{-}/\text{-}\ HIF\text{-}2\alpha\text{-}/\text{-}}$ than to parental cells. B) Compound **1** prolonged the lifespan of *C. elegans*. DMSO was used as control. $*p < 0.05$, $**p < 0.005$.

Experimental Section

General chemicals and bacterial strains: Molecular biology reagents and enzymes were purchased from Fisher Scientific. Primers were ordered from Sigma-Aldrich. Other chemicals and solvents were purchased from Sigma–Aldrich and Fisher Scientific. DNA sequencing was performed at Eurofins. A Shimadzu Prominence UHPLC system (Kyoto, Japan) fitted with an Agilent Poroshell 120EC-C18 column (2.7 μm, 3.0×50 mm), coupled with a PDA detector was used for HPLC analysis. For semi-preparative HPLC, YMC-Pack Ph column (5 μm, 4.6×250 mm) was used. NMR spectra of compound **1** were recorded in [D_6]acetone on a Bruker 400 MHz instrument, and a Bruker 600 MHz spectrometer was used to record its 1D NMR data in CD_3OD at - 20 °C and in [D_6]DMSO. NMR spectra of compound **2** were recorded in CD_3OD at - 20 °C on a Bruker 600 MHz spectrometer, while those of **3** were recorded in [D_6] DMSO on a Bruker 600 MHz spectrometer using a 5-mm TXI Cryoprobe. NMR instruments were located in the AMRIS facility at the University of Florida, Gainesville, FL, USA. Spectroscopy data were collected using Topspin 3.5 software. HRMS data were obtained using a Thermo Fisher Q Exactive Focus mass spectrometer equipped with an electrospray probe on Universal Ion Max API source.

Strain isolation and identification: The samples of black band mat used in this study were collected from Looe Key reef in Florida on July 9th, 2014. The samples were cut into small segments and rinsed with sterile artificial seawater three times to eliminate adherent surface debris. Pieces of the sample were immersed in 70% EtOH for one to two min for surface sterilization. After drying with sterile cotton cloth, the pieces were placed on the surface of potato dextrose broth (PDB, BD). The agar plates sealed with parafilm were incubated at 30 °C for two weeks. Individual strains were isolated by transferring hyphal tips growing out of the cut tissue pieces onto the fresh PDB supplementing with antibiotics. The pure fungus strain *P. steckii* YE was isolated after several rounds of purification with antibiotics. Taxonomic identification of the fungal strain was achieved by PCR amplification using the primer pair ITS1 and ITS4. Genomic DNA isolation followed the standard protocol,[18] including cell lysis, digestion of RNA by RNAse A, removal of precipitates and cell debris, DNA precipitation and purification. PCR amplicons (~550 bp) were purified and sequenced with the primer ITS1. BLAST analysis was performed for taxonomic identification. The sequence was deposited in GenBank (KY750301).

Fungal genome isolation and sequencing: *P. steckii* YE was cultured in 50 mL liquid PDB (Difco™ Potato Dextrose Broth, BD) prepared with artificial seawater at 30 °C for one week. Fungal

mycelia were collected by filtration and the fungal genomic DNA was isolated with MasterPure Yeast DNA Purification kit (Epicentre Biotechnologies) as described in the manual. Quality control and sequencing analysis were performed by Beijing Genome Institute (BGI) Genomics. Sequencing was conducted using Illumina Hi-seq4000. We used two types of libraries, one pair-end library with an insert size of less than 800 bp and one mate-end library with an insert size of 5–6 kb. Quality control and filtering of sequencing data were conducted using the FAstQc tool with a cutoff Phred quality score of $\geq$25. This process yielded a total of 12121754 paired-end reads and 17939608 mated-end reads with 150 bp length on average. Genome assembly was performed using Spades V3.11 using kmer sizes of 213355 and 77.[19] Assembled contigs were corrected and polished by mapping against the Illumina reads and calling errors using Pilon correction tool.[20] The procedure was repeated twice. Polished assembled contigs shorter than 1 kb and with biased read coverage were filtered and discarded. The final assembly produced a genome of 33183796 bp covered by 781 contigs ($\geq$1 kb). The max sequence length was 579389 bp and the N50 was 162,651 bp. The average read coverage for contig was 109 X, with a GC content of 45.9%. The nucleotide sequence of the gliotoxin cluster was used as a query in a blastn search to identify a 53-kb gene cluster potentially responsible for the biosynthesis of identified ETPs. The Genbank accession number of this cluster is MT489695.

Fungal culturing and ETP isolation: The isolated fungal strain was subcultured in 5 mL PDB prepared in artificial seawater (SWPDB) at 28 °C, 250 rpm for three days and then inoculated in 50 mL SWPDB to grow under the same conditions. After 7 days, the above-mentioned fungal culture was used to inoculate eight 2-L flasks, each containing 500 mL SWPDB. The fermentation was performed at 28 °C, 250 rpm for 7–14 days. The fungal culture medium was then filtered and extracted with EtOAc three times. The collected fungal mycelium was also extracted by EtOAc three times. EtOAc extracts were combined, washed with MQ water, dried over anhydrous Na_2SO_4 and finally filtered through the sintered funnel. The filtrate was concentrated to dryness *in vacuo* to afford 1.6 g crude extract. The crude extract was fractionated by silica gel column with increasing polarity from dichloromethane to MeOH to yield eight fractions (Frs. 1–8) based on TLC analysis. Fr. 2 (96 mg) was redissolved in 3 mL methanol for semi-preparative HPLC with a semi-prep column (Agilent ZORBAX SB-C_{18}, 5 μm, 9.4×250 mm or YMC-Pack Ph, 5 μm, 4.6×250 mm). Adametizine A (**1**; 15.2 mg), penigainamide A (**2**; 1.0 mg), penigainamide B (**3**; 0.2 mg) and FA-2097 (**4**; 1.2 mg) were purified by this way.

Detection of adametizine A (1) in black band layer samples: About 10 g of collected samples of black band layers were lyophilized for 8 h and then suspended in 15 mL methanol at 21 °C, 250 rpm for 3 h. The sample was centrifuged at 3000 rpm on the SX4750A rotor of Beckman Allegra X-15R for 5 min, and the clear supernatant was transferred and evaporated to dryness *in vacuum*. The dried residue was dissolved in 0.5 mL LC-MS methanol and centrifuged at 15000 rpm, room temperature for 30 min. The supernatant (10 μL) was subjected to HPLC and LC-MS analysis.

Adametizine A (1): Colorless solid; $[\alpha]_D^{20}$ = - 180 (*c* 0.067, MeOH); HRMS (ESI-TOF) *m/z* 531.0660 $[M+H]^+$ (calcd. for $C_{21}H_{24}ClN_2O_8S_2$, 531.0657); ^1H and ^{13}C NMR ([D_6]acetone, 400 MHz), Table S1. Single crystals of **1** were obtained by slow evaporation from dioxane and hexane at room temperature. X-ray intensity data were collected at 100 K on a Bruker DUO diffractometer using $Mo_{K\alpha}$ radiation (α = 0.71073 Å) and an APEXII CCD area detector. Raw data frames were read by program SAINT and integrated using 3D profiling algorithms. The structure was solved and refined in *SHELXTL2014*, using full-matrix least-squares refinement. The non-H atoms were refined with anisotropic thermal parameters and all of the H atoms were calculated in idealized positions and refined riding on their parent atoms. In addition to the molecule, there is one dioxane molecule in the asymmetric unit. The crystallographic data were deposited at the Cambridge Crystallographic Data Centre (CCDC 1556134).

Penigainamide A (2): Colorless solid; $[\alpha]_D^{20}$ = - 281 (*c* 0.027, MeOH); ECD (*c* 0.01, MeOH) λ_{max} 216 (- 3.85) and 262 (- 2.56); HRMS (ESI-TOF) *m/z* 563.0233 $[M+H]^+$ (calcd for $C_{21}H_{24}ClN_2O_8S_3$, 563.0383); ^1H and ^{13}C NMR were carried out at - 20 °C (CD_3OD, 600 MHz), Table S2.

Penigainamide B (3): Colorless solid; $[\alpha]_D^{20}$ = - 45 (*c* 0.0067, MeOH); HRMS (ESI-TOF) *m/z* 463.1158 $[M+H]^+$ (calcd for $C_{21}H_{23}N_2O_8S$, 463.1175); ^1H and ^{13}C NMR ([D_6]DMSO, 600 MHz), Table S3.

Cell viability assay: MTT assay was performed using HeLa, PC-3, LNCaP, parental HCT116, and HCT116$^{HIF\text{-}1\alpha\text{-}/\text{-}\ HIF\text{-}2\alpha\text{-}/\text{-}}$ cells. The HCT116 parental and knockout cells and the PC-3 and LNCap cells were cultured in Dulbecco's modified Eagle's medium (DMEM) or Roswell Park Memorial Institute Medium (rpmI1640) containing 10% fetal bovine serum and 100 U/mL penicillin and streptomycin and maintained at 37 °C in a humidified incubator under 5% CO_2. The cells (PC-3, 5×10^3; LNCaP, HCT116 parental and knockout cells 8×10^3; HeLa, 10^4 cells/well) were seeded onto a 96-well plate and incubated overnight. Varying concentrations of purified adametizine A (**1**; up to 100 μM) were added to the wells. After incubation at 37 °C for 48 or 72 h (HeLa), the cell viability was determined by MTT kit (Promega), following manufacture's protocols. Alternatively, 10 μL of MTT (five mg/mL) in PBS was added and incubated for 4 h, followed by the aspiration of the medium. Dimethyl sulfoxide (DMSO, 100 μL) was added to each well to dissolve the MTT in the wells and the plate was agitated for 1 h. The optical density (OD) was measured at 570 nm using a UV/vis microplate spectrophotometer (BioTek or Spectramax). Three to six replications were performed per treatment. The IC_{50} value was determined by analyzing data with Excel or GraphPad Prism 5 (GraphPad Software, Inc.).

Acknowledgements

This study was supported by the National Institutes of Health grants R35GM128742 (Y.D.), R01CA172310 (H.L.) and R50CA211487 (R.R.). Collection of black band disease samples was supported by Mote Protect our Reefs grant (POR 2013–2), and with NOAA FKNMS permit # FKNMS-2015-078-A1. We thank Jim Rocca, Dake Liu, Guqin Shi, Verrill M. Norwood IV, Weijing Cai and Profs. Steven Bruner and Chao Jiang for technical assistance and insights. NMR spectra were taken at Advanced Magnetic Resonance Imaging and Spectroscopy Facility at the University of Florida.

Conflict of Interest

The authors declare no conflict of interest.

Keywords: antiaging · biosynthesis · chemical transformation · cytotoxicity · epithiodiketopiperazine

[1] T. R. Welch, R. M. Williams, *Nat. Prod. Rep.* **2014**, *31*, 1376–1404.
[2] D. H. Scharf, T. Heinekamp, N. Remme, P. Hortschansky, A. A. Brakhage, C. Hertweck, *Appl. Microbiol. Biotechnol.* **2012**, *93*, 467–472.
[3] a) P. Klausmeyer, T. G. McCloud, K. D. Tucker, J. H. Cardellina II, R. H. Shoemaker, *J. Nat. Prod.* **2005**, *68*, 1300–1302; b) Y. Liu, A. Mandi, X. M. Li, L. H. Meng, T. Kurtan, B. G. Wang, *Mar. Drugs* **2015**, *13*, 3640–3652; c) C. Miyamoto, K. Yokose, T. Furumai, H. B. Maruyama, *J. Antibiot.* **1982**, *35*, 374–377; d) P. Seephonkai, P. Kongsaeree, S. Prabpai, M. Isaka, Y. Thebtaranonth, *Org. Lett.* **2006**, *8*, 3073–3075; e) R. D. Stipanovic, C. R. Howell, *J. Antibiot.* **1982**, *35*, 1326–1330; f) R. S. Orfali, A. H. Aly, W. Ebrahim, M. S. Abdel-Aziz, W. E. G. Müller, W. Lin, G. Daletos, P. Proksch, *Phytochem. Lett.* **2015**, *11*, 168–172; g) Y. Liu, X. M. Li, L. H. Meng, W. L. Jiang, G. M. Xu, C. G. Huang, B. G. Wang, *J. Nat. Prod.* **2015**, *78*, 1294–1299; h) M. Kajula, J. M. Ward, A. Turpeinen, M. V. Tejesvi, J. Hokkanen, A. Tolonen, H. Hakkanen, P. Picart, J. Ihalainen, H. G. Sahl, A. M. Pirttila, S. Mattila, *J. Nat. Prod.* **2016**, *79*, 685–690.
[4] P. Chankhamjon, D. Boettger-Schmidt, K. Scherlach, B. Urbansky, G. Lackner, D. Kalb, H. M. Dahse, D. Hoffmeister, C. Hertweck, *Angew. Chem. Int. Ed.* **2014**, *53*, 13409–13413; *Angew. Chem.* **2014**, *126*, 13627–13631.
[5] S. P. Gunasekera, J. L. Meyer, Y. Ding, K. A. Abboud, D. Luo, J. E. Campbell, A. Angerhofer, J. L. Goodsell, L. J. Raymundo, J. Liu, T. Ye, H. Luesch, M. Teplitski, V. J. Paul, *J. Nat. Prod.* **2019**, *82*, 111–121.
[6] Y. Jang, N. Huh, J. Lee, J. S. Lee, G. H. Kim, J. J. Kim, *Holzforschung* **2011**, *65*, 265–270.
[7] A. N. Yurchenko, O. F. Smetanina, E. V. Ivanets, A. I. Kalinovsky, Y. V. Khudyakova, N. N. Kirichuk, R. S. Popov, C. Bokemeyer, G. von Amsberg, E. A. Chingizova, S. Afiyatullov, S. A. Dyshlovoy, *Mar. Drugs* **2016**, *14*.
[8] a) P. J. Curtis, D. Greatbanks, B. Hesp, A. F. Cameron, A. A. Freer, *J. Chem. Soc. Perkin Trans. 1* **1977**, *2*, 180–189; b) M. Wang, Y. Hu, B. Sun, M. Yu, S. Niu, Z. Guo, X. Zhang, T. Zhang, G. Ding, Z. Zou, *Org. Lett.* **2018**, *20*, 1806–1809.
[9] H. R. Kilgore, C. R. Olsson, K. A. D Angelo, M. Movassaghi, R. T. Raines, *J. Am. Chem. Soc.* **2020**, 142, 15107–15115.
[10] a) R. J. Capon, *Nat. Prod. Rep.* **2020**, *37*, 55–79; b) A. A. Salim, K. Samarasekera, Z. G. Khalil, R. J. Capon, *Org. Lett.* **2020**, *22*, 4828-4832.
[11] P. D. Sherkhane, R. Bansal, K. Banerjee, S. Chatterjee, D. Oulkar, P. Jain, L. Rosenfelder, S. Elgavish, B. A. Horwitz, P. K. Mukherjee, *ChemistrySelect* **2017**, *2*, 3347–3352.
[12] a) R. R. Forseth, E. M. Fox, D. Chung, B. J. Howlett, N. P. Keller, F. C. Schroeder, *J. Am. Chem. Soc.* **2011**, *133*, 9678–9681; b) D. H. Scharf, J. D. Dworschak, P. Chankhamjon, K. Scherlach, T. Heinekamp, A. A. Brakhage, C. Hertweck, *ACS Chem. Biol.* **2018**, *13*, 2508–2512.
[13] M. S. Bousquet, J. J. Ma, R. Ratnayake, P. A. Havre, J. Yao, N. H. Dang, V. J. Paul, T. J. Carney, L. H. Dang, H. Luesch, *ACS Chem. Biol.* **2016**, *11*, 1322–1331.
[14] R. Ratnayake, S. P. Gunasekera, J. J. Ma, L. H. Dang, T. J. Carney, V. J. Paul, H. Luesch, *ChemBioChem* **2020**, *21*, 2356–2366.
[15] D. S. Wilkinson, R. C. Taylor, A. Dillin, *Methods Cell Biol.* **2012**, *107*, 353–381.
[16] C. J. Kenyon, *Nature* **2010**, *464*, 504–512.
[17] N. Boyer, K. C. Morrison, J. Kim, P. J. Hergenrother, M. Movassaghi, *Chem. Sci.* **2013**, *4*, 1646–1657.
[18] T. H. Al-Samarrai, J. Schmid, *Lett. Appl. Microbiol.* **2000**, *30*, 53–56.
[19] A. Bankevich, S. Nurk, D. Antipov, A. A. Gurevich, M. Dvorkin, A. S. Kulikov, V. M. Lesin, S. I. Nikolenko, S. Pham, A. D. Prjibelski, A. V. Pyshkin, A. V. Sirotkin, N. Vyahhi, G. Tesler, M. A. Alekseyev, P. A. Pevzner, *J. Comput. Biol.* **2012**, *19*, 455–477.
[20] B. J. Walker, T. Abeel, T. Shea, M. Priest, A. Abouelliel, S. Sakthikumar, C. A. Cuomo, Q. Zeng, J. Wortman, S. K. Young, A. M. Earl, *PLoS One* **2014**, *9*, e112963.

Manuscript received: June 23, 2020
Revised manuscript received: August 19, 2020
Accepted manuscript online: August 20, 2020
Version of record online: September 30, 2020

